Enhancement of Dispersion of Carbon Nanotube and Physical Properties of Poly(styrene-*co*-acrylonitrile)/ Multiwalled Carbon Nanotube Nanocomposite via Surface Initiated ATRP

Won Seok Choi, Sung Hun Ryu

Department of Chemical Engineering, College of Engineering, Industrial Liaison Research Institute, Green Energy Center, Kyung Hee University, Yongin, Korea

Received 10 September 2009; accepted 28 November 2009
DOI 10.1002/app.31921
Published online 28 January 2010 in Wiley InterScience (www.interscience.wiley.com).

ABSTRACT: Dispersion behavior of multiwalled carbon nanotube (MWCNT), rheological and mechanical properties of various MWCNT/poly(styrene-*co*-acrylonitrile) (SAN) nanocomposites were investigated. MWCNT/SAN nanocomposites were prepared by three different methods; MWCNT/SAN melt blending, MWCNT/SAN *in situ* atom transfer radical polymerization (ATRP) and functionalized-MWCNT/SAN *in situ* ATRP. Formation of SAN onto the surface of MWCNT and the molecular weight of grafted-SAN were confirmed by fourier transform infrared spectra, ^{1}H-NMR and ^{13}C-NMR. Crossover frequency of storage and loss modulus from rheological measurement and dynamic mechanical analysis showed that functionalized MWCNT/SAN *in situ* ATRP nanocomposite showed more uniform dispersion of MWCNT. Improved mechanical and electrical properties were observed for functionalized MWCNT/SAN *in situ* ATRP nanocomposite. © 2010 Wiley Periodicals, Inc. J Appl Polym Sci 116: 2930–2936, 2010

Key words: multiwalled carbon nanotube; dispersions; SAN; atom transfer radical polymerization (ATRP); nanocomposites

INTRODUCTION

Multiwalled carbon nanotube (MWCNT) has been attracted as a filler with polymeric materials to enhance mechanical and electrical properties. Recently CNTs have been used to reinforce various polymer, including polystyrene, poly(methyl methacrylate), poly(styrene-*co*-acrylonitrile) (SAN).[1–4] However, manipulation of MWCNT is limited by aggregation and poor dispersion in polymer matrix. Furthermore, poor interfacial adhesion between MWCNT and polymer matrix lowers efficient load transfer between matrix and MWCNT, which results in low mechanical properties. Functionalization or modification of the MWCNT surface has become a major activity to improve dispersibility and compatibility.[5–10] Grafting macromolecules onto CNTs have been explored for several years and significant works have been done in attaching macromolecules to the tips and convex walls of CNT's via special reactions such as etherification, amidization, radical coupling or other reactions.[9–11] However, prerequisite for this approach is that the macromolecules must possess suitable reactive functional sites. Recently the "grafting from" approach has been employed to functionalize MWCNT by *in situ* grafting polymer chains densely onto the convex wall of CNTs. Many linear polymers such as polystyrene (PS),[12,13] poly(methyl methacrylate) (PMMA),[14,15] polyimide,[16] poly(ethylene glycol),[17] SAN,[18] poly(vinyl alcohol) and its related copolymer poly(vinyl acetate-*co*-vinyl alcohol)[19] and hyperbranched polymers[20] have been successfully bonded onto CNTs.

Atom transfer radical polymerization (ATRP) has been proposed as most successful route of controlled radical polymerization and allows developing polymers with interesting functionalities and architectures. ATRP has been used to modify variety of silica surfaces[21–23] as well as pores of SBA-15[24] by growing polymer chains. ATRP also has been used in modifying the surfaces of gold,[25,26] magnetic nanoparticles,[27,28] and CdS nanoparticles.[29] Recently ATRP has been used extensively to functionalize the carbon nanotube by developing polymer brushes on the surface of nanotubes.[18,30,31] Wang et al. reported that PMMA grafted MWCNT increased mechanical properties, such as Young's modulus and tensile strength.[31] Similarly Shanmugharaj grafted SAN onto the surface of MWCNT and obtained improved dispersion behavior in tetrahydrofuran (THF).[18]

Correspondence to: S. H. Ryu (shryu@khu.ac.kr).
Contract grant sponsor: National Research Foundation of Korea; contract grant number: KRF-2007-D00144.

In this work, effect of functionalization of MWCNT and methods of MWCNT/SAN nanocomposite are investigated. Effective functionalization of MWCNT has been made by grafting SAN using ATRP and various properties, such as mechanical, rheological and electrical properties, are measured.

EXPERIMENTAL

Materials

MWCNT (NC 7000) used for this study was purchased from Nanocyl (Belgium). Styrene, acrylonitrile(AN), cuprous bromide (CuBr), 2-bromoisobutyrl bromide, thionyl chloride ($SOCl_2$), *N*,*N*,*N*′,*N*″,*N*″-pentamethyldiethylenetriamine (DETA), triethylamine (TEA) and ethylene glycol, anhydrous THF, ethanol, toluene were obtained from Aldrich Chemical company. Potassium hydroxide was obtained from standard local agent.

Surface initiated ATRP on MWCNT

In a typical polymerization, 50 mg of 2-hydroxyethyl bromoisobutyrate grafted MWCNT (0.016 mmol) was placed in a clean glass ampoule attached with a septum adaptor which was connected to both nitrogen and a vacuum system. 2-hydroxyethyl bromoisobutyrate grafted MWCNT (I-MWCNT) was prepared as described in previous work.[18] Styrene (0.075 mole) and acrylonitrile (0.025 mole) were added to the ampoule and solution of CuBr (0.1 mL, 0.016 mmol) and ligand ([CuBr]; [L] = 1 : 2) in toluene were added into the ampoule with a syringe under nitrogen atmosphere. Then the entire solution was degassed four times and sealed off under vacuum. The sealed ampoule was placed in an oil bath that was maintained at 80°C for 24 hr. It was observed that solution became viscous and tended to stick to walls of the ampoule after 4 hr. After 24 h, ampoule was quenched with liquid nitrogen and then the ampoule was opened. The heterogeneous polymerization solution was diluted with THF (20 mL) and kept under stirring in a round bottomed flask for few hours to dissolve soluble polymer. SAN-*g*-CNT were recovered as lumpy aggregates and dried at 40°C for 24 h under vacuum. The filtrate that contained the slightly grayish polymer was recovered by precipitation in methanol.

Preparation of SAN/MWCNT nanocomposite

SAN/MWCNT nanocomposites were prepared with three different methods. Composite A was prepared by simple melt blending of pristine MWCNT (P-MWCNT) and SAN which was synthesized at same conditions for SAN-*g*-MWCNT. Melt blending was performed using internal mixer (Sin-A, Korea) with sigma type rotor for 10 min at 210°C. Composites through P-MWCNT or I-MWCNT/SAN *in situ* polymerization as described earlier were designated as Composite B and Composite C, respectively.

Characterizations

Thermogravimetric analysis (TGA) of pure and functionalized carbon nanotube was done under nitrogen environment using Perkin–Elmer thermogravimetric analyzer (TGA 7) in the range of 50–800°C at a heating rate of 10°C/min. Fourier transform infrared spectra (FTIR) were recorded using Perkin–Elmer FTIR 2000 spectrometer in the range of 400– 4000 cm^{-1} at the resolution of 4.0 cm^{-1}. Structural characterization of polymer which was grafted onto MWCNT was done using 300 MHz ^{1}H and ^{13}C-NMR (JNM–AL 300, JEOL, Japan) with $CDCl_3$ as a solvent. The surface morphology of MWCNT was observed using transmission electron microscope (TEM) (JEM 2010, JEOL). TEM samples were prepared on the 400 mesh copper grid coated with carbon. Dynamic mechanical analysis (DMA) was performed using Dynamic Mechanical Thermal Analyzer (DMA 242C, Netchz). The samples were heated from 40 to 150°C at a heating rate of 10°C min^{-1}. Melt rheological measurements were performed in dynamic mode using ARES FRT 2000 (Rheometrics) with parallel plate geometry at 230°C under nitrogen atmosphere. Gel permeation chromatography (GPC, Waters 515 HPLC) was used to measure the molecular weight and molecular weight distribution of SAN. Temperature was 40°C and solution flow rate was 1.0 cc/min.

Stress–strain measurements were performed on a universal tensile tester (LF plus, Lloyd instruments) at room temperature with a crosshead speed of 5 mm/min. Compression molded specimen was used for this test and more than three different samples were used to obtain the data and results were quite reproducible. Room temperature electrical conductivity of the composite films was measured using the two probe technique in KEITHLEY 2000 digital multimeter.

RESULTS AND DISCUSSION

Figure 1 shows the FTIR spectra of pristine MWCNT (P-MWCNT), 2-hydroxyethyl bromoisobutyrate grafted MWCNT (I-MWCNT) and SAN-*g*-MWCNT. FTIR spectrum of I-MWCNT exhibits new peaks at 2920, 2880 and at 1735 cm^{-1} which represent —CH asymmetric and symmetric stretching of $—CH_2$ group and ⟩C=O stretching of —COO group in grafted hydroxyethyl isobutryl bromide onto the MWCNT surface as previous work.[18] Spectrum of

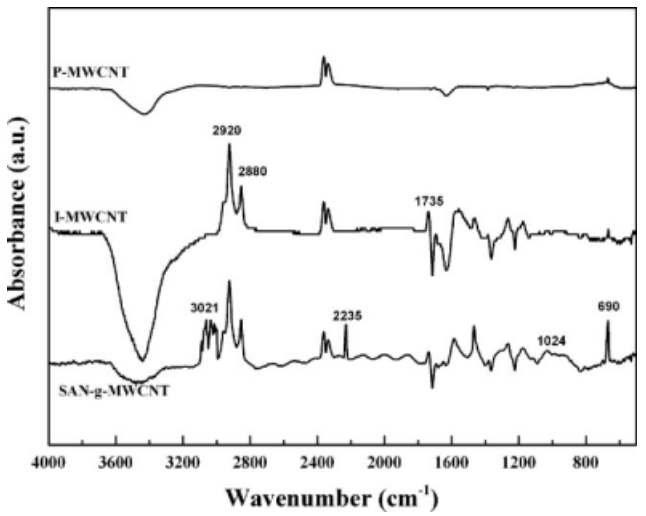

Figure 1 FTIR spectra of various MWCNTs.

SAN-*g*-MWCNT shows typical characteristic peaks of styrene and acrylonitrile. The appearance of peaks at 3021, 2920, 1024, and 690 cm^{-1}, which correspond to —CH stretching of aromatic ring, —CH asymmetric stretching of $—CH_2$ group, —C—O stretching of ester group in ATRP initiator and aromatic C—H out of plane bending vibration of styrene group. Peak at 2235 cm^{-1} represents the nitrile group of AN. From FTIR spectra, it is confirmed that initiator and SAN are successfully grafted on to MWCNT.

FTIR characterization does not give much information about the grafted-SAN which is grated onto the surface of MWCNT. To understand the characteristics of grafted-SAN, such as molecular weight and composition ratio, ^{1}H and ^{13}C-NMR characterizations are performed and results are shown in Figure 2. Broad signals in ^{1}H-NMR spectrum are due to the residual metallic catalyst and local field effects due to MWCNT[1] along with the signals due to the individual protons of MWCNT. ^{1}H-NMR spectrum shows peaks at 0.8, 1.2 ($—CH_3$ group in the initiator), 2.2 ($—CH_2$ groups in the initiator), 2.4 (—CH group of acrylonitrile), 6.7, 7.1 ppm (aromatic ring of styrene) and this result agrees with previous works.[2,3] Number average molecular weight (M_n) of grafted-SAN can be calculated with number of styrene unit from ^{1}H-NMR and the value of M_n is 49,300. It is common to determine the average monomer composition of copolymers with ^{1}H-NMR. However, the resolution of ^{1}H-NMR spectrum in the range of 1.2–3.2 ppm is not clear enough to identify the methylene and methane protons of grafted-SAN due to overlapping. For this reason, ^{13}C-NMR is used to determine grafted-SAN's average chemical composition of styrene and acrylonitrile unit. The nitrile carbon peaks are shown at 120–121.4 ppm (B), while the aromatic ring carbon of styrene group appears at 127–128 ppm and 137 ppm (A).[32] The relative peak areas of A and B can be used to calculate the average chemical composition of styrene and AN. Through NMR analysis it is found that chemical composition of [styrene]/[acrylonitrile] ratio in grafted-SAN is 75/25. Even though it is not easy to calculate the molecular weight distribution of grafted-SAN using NMR analysis, it can be inferred from the comparison of molecular weight and composition ratio of SAN without CNT and grafted-SAN of SAN-*g*-CNT which are synthesized at same conditions. M_n of SAN using GPC and NMR is 51,000 and 50,200, respectively. This indicates that NMR analysis is quite reliable to measure the M_n of SAN. Weight average molecular weight and molecular weight distribution of SAN using GPC are 113,200 and 2.22, respectively. It is also found that composition ratio (styrene/AN) of SAN is also quite close to grafted-SAN. From close M_n and composition ratio of SAN and grafted-SAN at same synthesis conditions, it is possible to infer that weight average molecular weight, i.e. molecular weight distribution, of SAN and grafted-SAN could be quite similar.

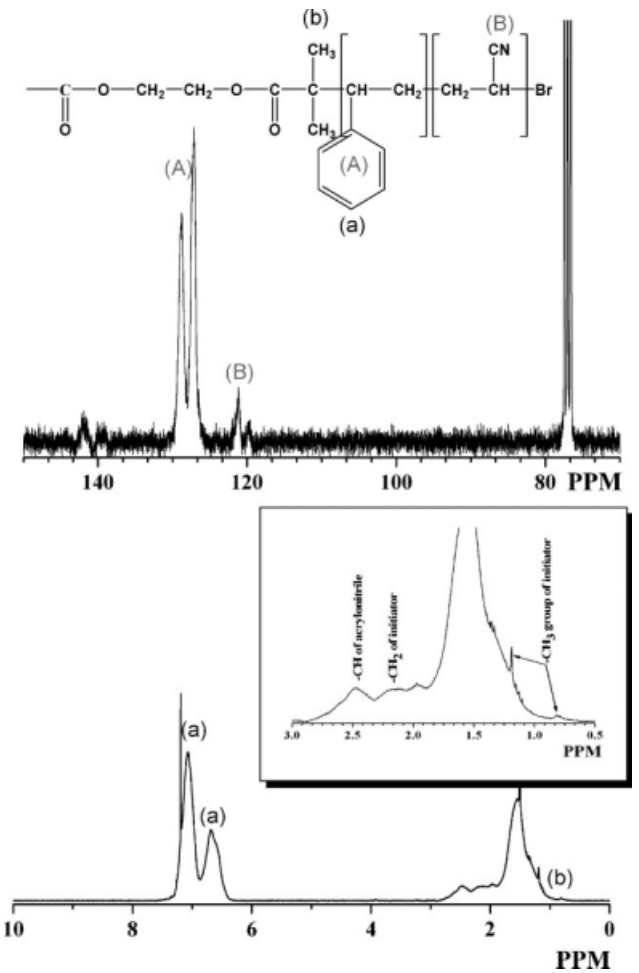

Figure 2 ^{1}H and ^{13}C-NMR spectra of SAN-*g*-MWCNT.

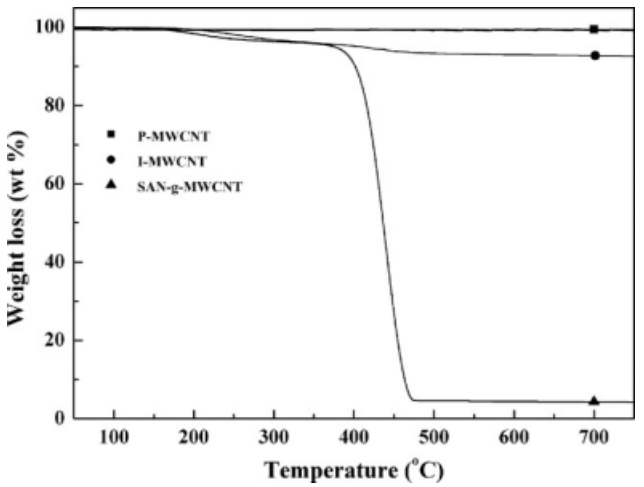

Figure 3 Thermogravimetric results of various MWCNTs.

Shown in Figure 3 is the TGA of P-MWCNT, I-MWCNT and SAN-*g*-MWCNT. P-MWCNT exhibits excellent stability up to 750°C, while I-MWCNT shows relatively significant loss. I-MWCNT starts to degrade from ca. 250°C and continues to degrade up to 500°C. 9.8 wt % of weight loss is observed at 750°C and it can be attributed to the presence of initiator. From the TGA results, a number of initiator introduced onto the surface of carbon nanotube can be calculated and it is found to be 3.8 initiators per 1000 carbon atoms and it is quite similar to previous work.[18] SAN-*g*-MWCNT shows significant weight loss at 360–380°C, which is close to the decomposition temperature of SAN copolymer reported by Wang et al.[31] and 98% weight loss is observed. This indicates that MWCNT is completely covered with SAN. TEM photographs in Figure 4 also confirm that SAN-*g*-MWCNT is covered with SAN completely.

Rheological behavior of SAN/MWCNT composite is examined to identify the effect of the SAN grafted onto the MWCNT. Figure 5 shows complex melt viscosity (η^*) of SAN and nanocomposites containing 2 wt % of MWCNTs. Complex melt viscosities of SAN and SAN nanocomposites decrease with increasing frequency, indicating typical non-Newtonian behavior over the whole frequency range. At low frequency range, the viscosity of composite C is five or three times higher than that of composite A or B, respectively. Composite C shows distinct shear thinning behavior compare to other composites. It has been known that better dispersion of CNTs results in higher shear viscosities and more distinct shear thinning behavior in CNT/polymer nanocomposites.[2,33] Thus, it can be concluded that composite C achieves better dispersion followed by composite B and A, respectively. Better dispersion of P-CNT in composite B compare to composite A can be attributed to the viscosity of medium during composite preparation. Composite B is prepared via *in situ* polymerization, which means P-CNT is dispersed in low viscosity styrene and AN mixture, while P-CNT is mixed with high viscosity SAN melt for composite A. The difference of viscosity of medium results in the difference of degree of dispersion.

Figure 6 shows the storage modulus (G') and loss modulus (G'') as a function of frequency and the values of G' and G'' increase with increasing frequency. Crossover frequencies between storage and loss modulus are observed for all samples and it indicates the presence of transition from liquid-like to solid-like behavior. SAN and nanocomposites show $G' < G''$ at low frequency terminal regime and

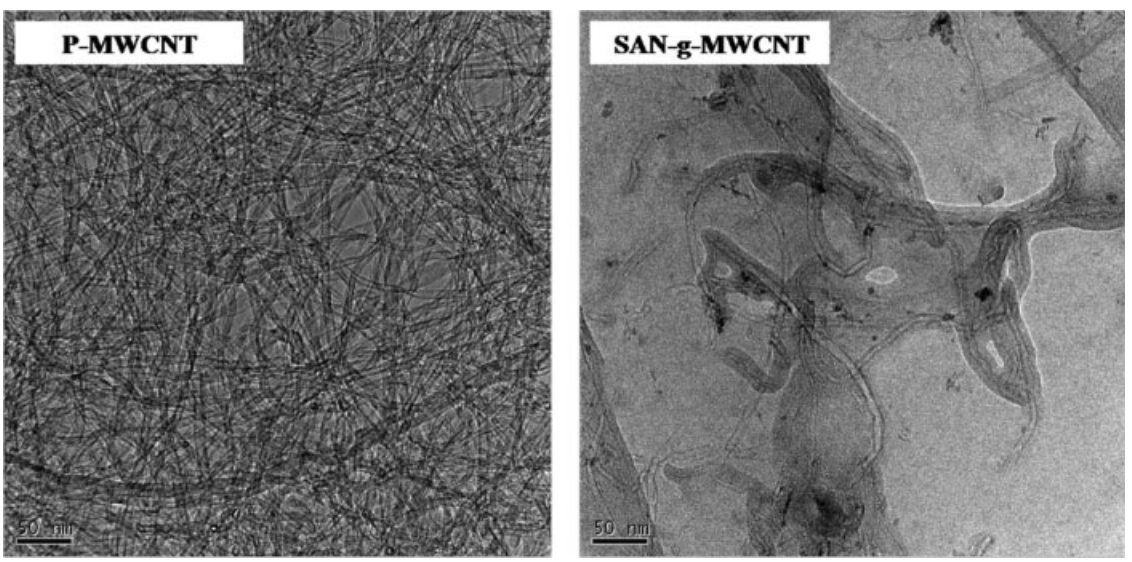

Figure 4 TEM photographs of P-MWCNT and SAN-*g*-MWCNT.

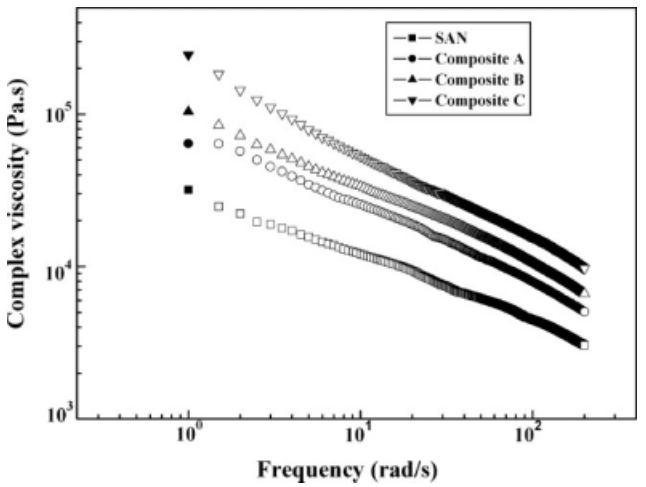

Figure 5 Complex viscosities of SAN and various SAN/MWCNT nanocomposites containing 2 wt % of MWCNT.

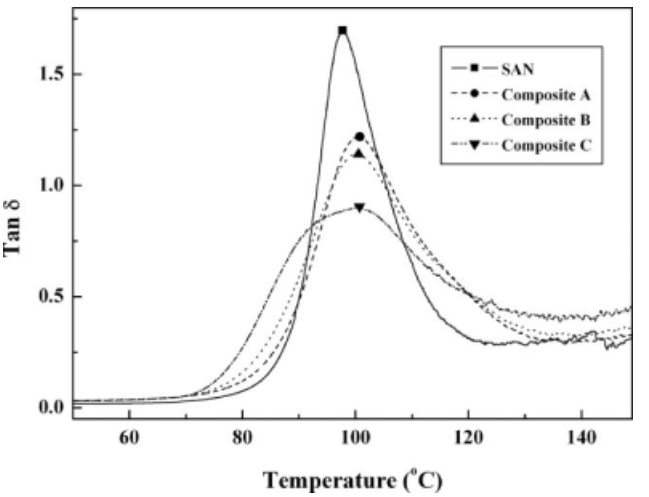

Figure 7 Tan δ curves of SAN and SAN nanocomposites.

crossover is observed at specific frequency after which $G' > G''$. It is well-known that lower crossover frequency and higher storage modulus than loss modulus indicates the solid-like behavior.[34,35] Composite C shows lowest crossover frequency at 0.8 S^{-1}, while composite A, B and SAN show 17, 16 and 69 S^{-1}, respectively. This result indicates that composite C acts as more solid-like behavior than others. The terminal slopes of G' of nanocomposites are 0.67, 0.62, 0.42 for composite A, B and C, respectively, and this nonterminal behavior also indicates that composite C shows more solid-like behavior.[33,35-37]

To understand the effect of *in situ* polymerization onto the surface of MWCNT, one must examine the interphase behavior and it can be well described by dynamic mechanical analysis. Figure 7 presents typical tan δ curves of SAN and nanocomposites as a function of temperature. The tan δ peak of SAN is observed at 97.7°C, while those of nanocomposites shift to higher temperatures. The presence of MWCNT can restrict the relaxation and motion of SAN molecules and it causes the shift of tan δ peak to higher temperatures and also decreases the peak intensity. Lowering peak height and broadening peak width indicate the better interfacial adhesion and dispersion.[38–40] From this result it is found that composite C shows better dispersion of CNT than composite B and also composite B exhibits better dispersion than composite A. This result confirms the above rheological data.

Figure 8 shows the typical stress–strain curves of nanocomposites. The tensile strength, strain and toughness of composite A are more or less same as SAN, while Young's modulus is improved by 23%. Low tensile strength and toughness can be attributed to higher degree of aggregation as well as weak interfacial interaction between MWCNT and SAN matrix.[41] Composite B and C show improved

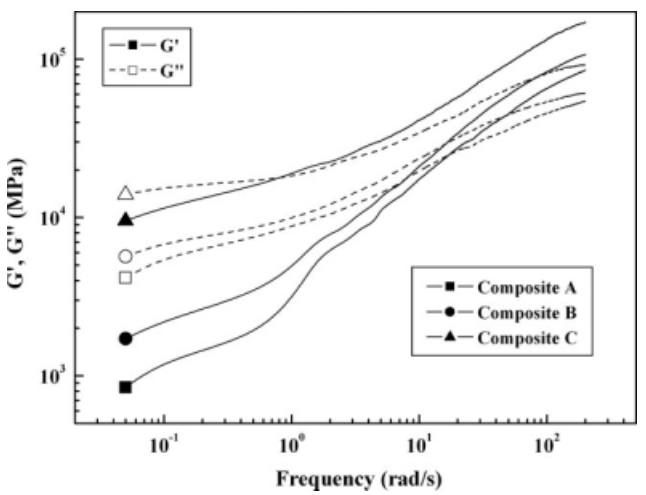

Figure 6 Storage (G') and loss modulus (G'') of SAN/MWCNT nanocomposites containing 2 wt % of MWCNTs.

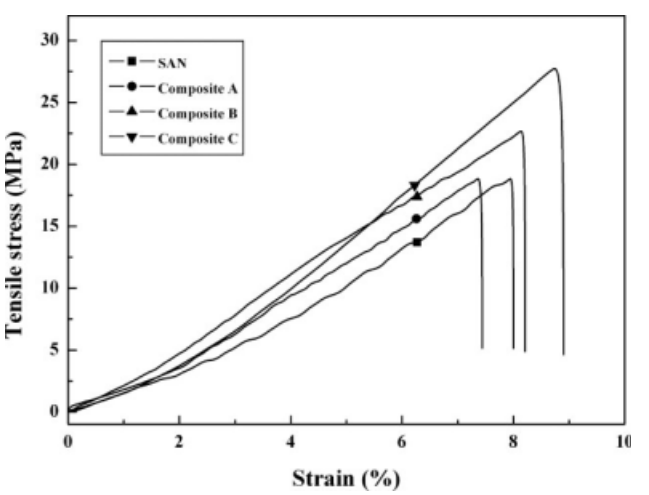

Figure 8 Tensile stress–strain curves of SAN and SAN/MWCNT nanocomposites.

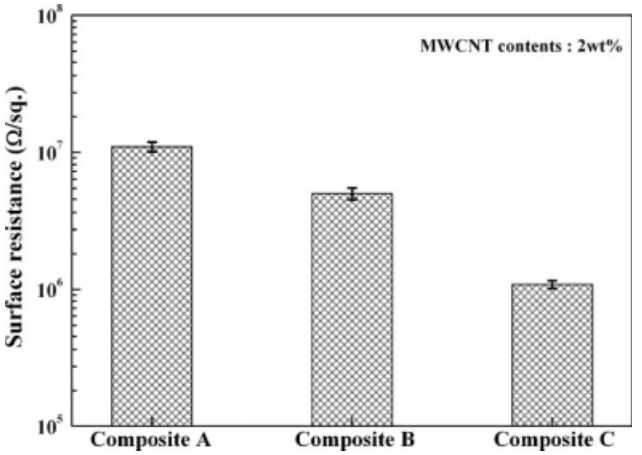

Figure 9 Surface resistance of MWCNT/SAN nanocomposites.

Young's modulus, tensile strength, strain and toughness. Especially, tensile strength and toughness of Composite C are significantly increased by 48 and 65% compared to SAN. In general, the incorporation of CNT to polymers enhances the mechanical property such as Young's modulus, but tensile strength and toughness tend to be very sensitive to the quality of the interfacial interaction and dispersion of the nanofiller for the materials of nanocomposites.[4,42] Excellent load transfer from matrix to filler is essential to achieve improved physical properties in polymer/filler composites. For composite C, SAN is directly grafted onto the surface of MWCNT via ATRP which will results in excellent interfacial load transfer. Thus in addition to the degree of dispersion as discussed earlier, improved interfacial characteristic is reason why composite C achieves significant increase in toughness, tensile strength and Young's modulus. Improved mechanical properties of composite B compare to composite A can be attributed to the better dispersion of MWCNT in composite B.

It is well known that dispersion state of MWCNTs in the polymer matrix affects electrical properties of polymer composites directly. Figure 9 shows the surface resistance of composites. Composite C shows lowest surface resistance by the one order of magnitude compare to composite A and B, while resistance of composite B is slightly lower than that of composite A.

CONCLUSIONS

The ATRP of SAN onto MWCNT was carried out via the introduction of an ATRP initiator onto the surface of MWCNT. The formation of grafted-SAN onto the surface of CNT was confirmed by FTIR, ^{1}H-NMR and ^{13}C-NMR. The degree of dispersion of MWCNT and mechanical and electrical properties of nanocomposites were investigated for MWCNT/SAN nanocomposites prepared by three different methods; P-MWCNT/SAN melt blending, P-MWCNT/SAN *in situ* ATRP and I-MWCNT/SAN *in situ* ATRP. I-MWCNT/SAN *in situ* ATRP, i.e. SAN-*g*-MWCNT, showed higher viscosity and broader tan δ peak compare to other nanocomposites which indicate improved dispersion of MWCNT and interfacial characteristics. Higher tensile properties and toughness and lowest electrical resistance was for SAN-*g*-MWCNT. These were attributed to the improved interfacial behavior and degree of dispersion of MWCNT.

References

1. Sabba, Y.; Thomas, E. L. Macromolecules 2004, 37, 4815.
2. Mitchell, C. L.; Bahr, J. L.; Arepalli, S. A.; Tour, J. M.; Krishnamoorti, R. Macromolecules 2002, 35, 8825.
3. Du, F.; Fischer, J. E.; Winey, K. I. J Polym Sci Part B: Polym Phys 2003, 41, 3333.
4. Wang, M.; Pramoda, K. P.; Goh, S. H. Polymer 2005, 46, 11510.
5. Ajayan, P. M. Chem Rev 1999, 99, 1787.
6. Hirsch, A. Angew Chem Int Ed 2002, 41, 1853.
7. Baughman, R. H.; Zakhidov, A. A.; De Heer, W. A. Science 2002, 297, 787.
8. Santos, C. V.; Martinez-Hernandez, A. L.; Fisher, F. T.; Ruoff, R.; Castano, V. M. Chem Mater 2003, 15, 4470.
9. Bianco, A.; Prato, M. Adv Mater 2003, 15, 1765.
10. Chen, J.; Hamon, M. A.; Hu, H.; Chen, Y.; Rao, A. M.; Eklund, P. C.; Haddon, R. C. Science 1998, 282, 95.
11. Riggs, J. E.; Guo, Z.; Carroll, D. L.; Sun, Y. P. J Am Chem Soc 2000, 122, 5879.
12. Sano, M.; Kamino, A.; Okamura, J.; Shinkai, S. Langmuir 2001, 17, 5125.
13. Homenick, C. M.; Sivasbramaniam, U.; Adronov, A. Polym Int 2008, 57, 1007.
14. Koshio, A.; Yudasaka, M.; Zhang, M.; Iijima, S. Nano Lett 2001, 1, 361.
15. Kong, H.; Gao, C.; Yan, D. Macromolecules 2004, 37, 4022.
16. Park, C.; Ounaies, Z.; Watson, K. A.; Crooks, R. E.; Smith, J.; Lowther, S. E.; Connell, J. E.; Siochi, E. J.; Harrison, J. S.; St. Clair, T. L. Chem Phys Lett 2002, 364, 303.
17. Kahn, M. G. C.; Banerjee, S.; Wong, S. S. Nano Lett 2002, 2, 1215.
18. Shanmugharaj, A. M.; Bae, J. H.; Nayak, R. R.; Ryu, S. H. J Polym Sci Part A: Polym Chem 2007, 45, 460.
19. Lin, Y.; Zhou, B.; Fernando, K. A. S.; Allard, L. F.; Sun, Y. P. Macromolecules 2003, 36, 7199.
20. Cao, L.; Yang, W.; Yang, J.; Wang, C.; Fu, S. Chem Lett 2004, 33, 490.
21. Pyun, J.; Kowalewski, T.; Matyjaszewski, K. Macromol Rapid Commun 2003, 24, 1043.
22. Ramakrishnan, A.; Dhamodharan, R.; Rühe, J. J Polym Sci Part A: Polym Chem 2006, 44, 1758.
23. Chen, R.; Feng, W.; Zhu, S.; Botton, G.; Ong, B.; Wu, Y. J Polym Sci Part A: Polym Chem 2006, 44, 1252.
24. Kruk, M.; Dufour, B.; Celer, E. B.; Kowalewski, T.; Jaroniec, M.; Matyjaszewski, K. J Phys Chem B 2005, 109, 9216.
25. Kim, J. B.; Bruening, M. L.; Baker, G. L. J Am Chem Soc 2000, 122, 7616.
26. Kotal, A.; Mandal, T. K.; Walt, D. R. J Polym Sci Part A: Polym Chem 2005, 43, 3631.
27. Vestal, C. R.; Zhang, Z. J. J Am Chem Soc 2002, 124, 14312.
28. Gravano, S. M.; Dumas, R.; Liu, K.; Patten, T. E. J Polym Sci Part A: Polym Chem 2005, 43, 3675.

29. Cui, T.; Zhang, J.; Wang, J.; Cui, F.; Chen, W.; Xu, F.; Wang, Z.; Zhang, K.; Yang, B. Adv Funct Mater 2005, 15, 481.
30. Baskaran, D.; Mays, J. M.; Bratcher, M. S. Angew Chem Inter Ed 2004, 43, 2138.
31. Wang, H. W.; Chang, K. C.; Chu, H. C. Polym Int 2005, 54, 114.
32. Al-Harthi, M.; Sardashti, A.; Soares, J. B. P.; Simon, L. C. Polymer 2007, 48, 1954.
33. Hu, G.; Zhao, C.; Zhang, S.; Yang, M.; Wang, Z. Polymer 2006, 47, 480.
34. Lele, A.; Mackley, M.; Galgali, G.; Ramesh, C. J Rheol 2002, 46, 1091.
35. Song, Y. S. Polym Eng Sci 2006, 46, 1350.
36. Kim, J. Y. J Appl Polym Sci 2009, 112, 2589.
37. Krishnamoorti, R.; Giannelis, E. P. Macromolecules 1997, 30, 4097.
38. Abdullah, S. A.; Iqbal, A.; Frormann, L. J Appl Polym Sci 2008, 110, 196.
39. Tsagaropoulos, G.; Eisenber, A. Macromolecules 1995, 28, 6067.
40. Kim, J. I.; Ryu, S. H.; Chang, Y. W. J Appl Polym Sci 2000, 77, 2595.
41. Jia, Z.; Wang, Z.; Xu, C.; Liang, J.; Wei, B.; Wu, D. Mater Sci Eng A 1999, 271, 395.
42. Coleman, J. N.; Cadek, M.; Blake, R.; Nicolosi, V.; Ryan, V. P.; Belton, C. Adv Funct Mater 2004, 14, 791.